CAVITATION TESTS OF HYDRAULIC MACHINES: PROCEDURE AND INSTRUMENTATION

François Avellan
IMHEF - Institut de Machines Hydrauliques et de Mécanique des Fluides
EPFL - Swiss Federal Institute of Technology,
Lausanne, Switzerland

ABSTRACT

Model testing of hydraulic turbines, storage pumps and pump-turbines is of great importance especially for large units involved in power generation. Among all the aspects of machine operation, cavitation plays a fundamental role with respect to the possible alteration of the efficiency and to the erosion risk. This paper describes the procedures of cavitation tests and the related special instrumentation, depending both on the type of hydraulic machine and its operation range. Discussion is mainly directed toward the unavoidable distortions of the similitude requirements between model and industrial scales. In particular, Froude similitude requires a test head of such a value, too high or too low, that it would be impossible to perform reasonable tests with respect to the Reynolds effect or to the limited capacity of the model and/or of the test installation. The influence of free stream nuclei content on the cavitation development is examined and the instrumentation related to the control of nuclei content is described. Recent developments in the evaluation of erosion risk allow to propose a new test procedure using solid borne noise measurements to infer local pressure fluctuations acting on the runner .

NOMENCLATURE

A	Flow passage cross section area		(m^2)
C	Mean flow velocity	$C = Q/A$	(ms^{-1})
Cm	Meridional component of the velocity		(ms^{-1})
Cu	Circumferential component of the velocity		(ms^{-1})
D	Reference diameter of the runner		(m)
E	Specific hydraulic energy	$E = gH_1 - gH_2$	(Jkg^{-1})
Fr	Froude number	$Fr = \sqrt{\frac{E}{gD}}$	
NPSE	Net Positive Suction Energy		(Jkg^{-1})
H_s	Setting level of the machine	$Hs = Z_T - Z_a$	(m)
P	Mechanical power of the machine		(W)
P_h	Hydraulic power	$P_h = \rho QE$	(W)
P_m	Mechanical power of the runner	$P_m = \omega T_m$	(W)
Q	Discharge		(m^3s^{-1})
Q_{ED}	Discharge factor according to IEC definition	$Q_{ED} = \frac{Q}{D^2 E^{\frac{1}{2}}}$	(-)
R	Reference radius of the runner	$R = D/2$	(m)
T_m	Torque acting on the runner		(Nm)
U	Circumferential velocity		(ms^{-1})
W	Relative velocity	$\vec{W} = \vec{C} - \vec{U}$	(ms^{-1})
Z	Elevation		(m)
Z_a	Elevation of the tail water level		(m)
Z_T	Reference elevation of the machine		(m)
c_p	Static pressure coefficient	$c_p = \frac{p - p_c}{\rho E}$	(-)
k	Geometric factor		(-)
g	Acceleration due to gravity		(ms^{-2})
gH	Mean specific energy of a flow passage cross section	$\frac{p}{\rho} + gZ + \frac{C^2}{2}$	(Jkg^{-1})
n	Speed of revolution		(s^{-1})
	Power law exponent of the nuclei radius distribution		(-)
n_{ED}	Speed factor according to IEC definition	$n_{ED} = \frac{nD}{E^{\frac{1}{2}}}$	(-)
p	Absolute static pressure		(Pa)
p_a	Atmospheric pressure		(Pa)
p_{va}	Vapor pressure		(Pa)
χ_E	Local cavitation factor	$\chi_E = \frac{p_c - p_{va}}{\rho E}$	(-)
ΔgH	Specific energy losses.		(Jkg^{-1})
$\Delta\psi$	Coefficient of energy losses	$\Delta\psi = \frac{2\Delta gH}{\omega^2 R^2}$	(-)
λ_E	Prototype to model energy ratio		(-)
λ_L	Prototype to model length scale		(-)

η	Efficiency		(-)
φ	Flow coefficient	$\varphi = \frac{Q}{\pi\omega R^3}$	(-)
φ_0	Whirl free flow coefficient		(-)
ρ	Water density.		(kg/m^3)
σ	Thoma number		(-)
σ_0	Lowest value of σ for which the efficiency remains unchanged as compared to cavitation free operation		
σ_1	Lowest value of σ as compared to cavitation free operation for which an efficiency drop of 1% is noticed		
ψ	Specific hydraulic energy coefficient	$\psi = \frac{2E}{\omega^2 R^2}$	(-)
ψ_c	Net positive suction specific hydraulic energy coefficient	$\psi_c = \frac{2NPSE}{\omega^2 R^2}$	(-)
ω	Angular velocity of the runner.		(rad/s)
1; 2,	Subscripts corresponding to the high pressure side and the low pressure side of the machine		
c	Subscript corresponding to the low pressure side of the runner		

INTRODUCTION

Model testing of hydraulic machines is of great importance especially for large units involved in power generation, [1]. The international community acknowledges this importance by editing recommendations through the International Electrotechnical Commission, IEC. Thus a revised version of the international code for model acceptance tests of hydraulic machines is presently submitted to each national committee and will be edited soon. Among all the aspects of machine operation, developed cavitation plays a fundamental role with respect to the possible alteration of the efficiency and to the erosion risk. Indeed, by reducing the machine dimensions and its setting level a machine operation under cavitation condition is economically preferable to cavitation free operation as far as the efficiency is unaffected and the erosion limited. This explains why the cavitation inception problem receives little attention in the case of hydraulic machines. Moreover, the need to perform cavitation tests of a hydraulic machine fully justifies to perform model testing with a special test rig in contrast to field tests for which the machine setting level is quite impossible to vary in a large extent.

The aim of this paper is to describe the procedures of cavitation tests and the related special instrumentation. However, depending on the type of hydraulic machine and its operation range, an appropriate procedure must be followed in order to be as similar as possible with the corresponding flow at the prototype scale. The discussion is mainly directed towards the unavoidable distortions of the similitude requirements. In particular, Froude similitude requires a test head of such a value, too high or too low, that it would be impossible to perform reasonable tests with respect to the Reynolds effect or to the limited capacity of the model and/or of the test installation. The influence of the free stream nuclei content on the cavitation development is examined through the practice of IMHEF for many years in performing cavitation nuclei control. The micro bubble injection system and the cavitation nuclei counter in use for this control is described and typical results are given in the case of Francis turbines.

Erosion risk evaluation can take advantage of the recent developments in this field. New trends in measuring this erosion risk are discussed. A test procedure is proposed by using the solid borne noise measurement to infer local pressure fluctuations acting on the blade and thus leading to the cavitation aggressiveness.

The general model test procedure of the hydraulic machines is first presented. Particular definition of the hydraulic operation parameters are given and similitude requirements are examined. In the second part, the cavitation aspects of different types of hydraulic machines are then discussed as related to the risks of the performance alteration and the erosion. In a third part, the influence of free stream cavitation nuclei on cavitation tests is detailed and the procedure of nuclei control is described with the related instrumentation. The erosion risk evaluation procedure is finally examined by discussing the vibratory characteristics of cavitation erosion.

MODEL TESTING OF HYDRAULIC MACHINES

General definition and notation

We examine in this paper the case of reaction hydraulic machines including hydro-turbine, storage pump or pump-turbine. Irrespective of the flow direction the subscript 1 defines the high pressure reference section of the machine and the subscript 2 the low pressure reference section, as defined in Figure 1.

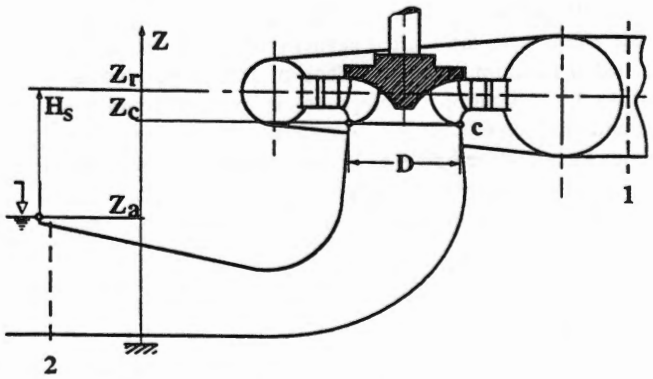

FIG. 1 GENERAL SKETCH OF A CENTRIFUGAL HYDRAULIC MACHINE.

The low pressure section of the runner is quoted with the subscript c. The specific hydraulic energy E of the machine is the one available between the high and the low pressure reference sections. By introducing p, the absolute pressure, Z, the elevation of a point and C the mean velocity defined by the

ratio between the discharge Q and the section area A, the specific hydraulic energy E is defined by:

$$E = \left[\frac{p_1}{\rho} + gZ_1 + \frac{C_1^2}{2}\right] - \left[\frac{p_2}{\rho} + gZ_2 + \frac{C_2^2}{2}\right] (Jkg^{-1})$$

where ρ is the water density and g the acceleration due to gravity. The hydraulic power P_h of the machine is then the product

$$P_h = \rho Q E \quad (W)$$

Since the mechanical power P of the machine includes the mechanical power dissipated in guide bearings, thrust bearings and shaft seals of the hydraulic machine, the mechanical power P_m of the runner is introduced. If T_m is the torque at the coupling of the runner and the shaft, P_m is:

$$P_m = \omega T_m \quad (W)$$

where ω is the angular velocity of the runner. The hydraulic efficiency is then defined as

$$\eta_h = \frac{P_h}{P_m} \text{ for a pump and } \eta_h = \frac{P_m}{P_h} \text{ for a turbine.}$$

Geometrical and kinematic similarity principles allow to define the dimensionless terms which determine the hydraulic characteristics of the machine. Two sets of reference quantities are usually used to define dimensionless terms. First, the rotational speed n, expressed in revolution per unit time, the reference diameter D and the specific hydraulic energy E define the speed factor n_{ED} and the discharge factor Q_{ED} as follow

$$n_{ED} = \frac{nD}{E^{\frac{1}{2}}} \quad , \qquad Q_{ED} = \frac{Q}{D^2 E^{\frac{1}{2}}} .$$

A second set of reference quantities consisting in the angular velocity ω, the reference radius R and the reference specific kinetic energy $(\omega R)^2/2$ leads to the definition of the energy coefficient ψ and the discharge coefficient φ.

$$\psi = \frac{2E}{\omega^2 R^2} \quad , \qquad \varphi = \frac{Q}{\pi \omega R^3} .$$

The last pair of coefficients can be preferably used since they are directly proportional to the specific energy E and the discharge Q. Efficiency hill charts expressed in terms of these coefficients present the same shape as those expressed as a function of E and Q. Thus, for a given hydraulic machine and a given angle of guide vanes, if any, the hydraulic efficiency can be written

$$\eta_h = \eta_h(\varphi, \psi, \alpha) .$$

For real flow, viscosity must be taken into account in order to achieve a full dynamic similarity of the flow in the hydraulic machine. In this case, the Reynolds number of the flow influences the efficiency. Then a transposition law from model to prototype scale has to be established in order to scale-up the hydraulic efficiency.

General test procedure

Model tests require that the geometric, the kinematic and the dynamic similitude principles are fulfilled between model and prototype. Model dimensions must be sufficient to achieve an excellent geometrical similarity with the prototype; the typical outlet diameter D of Francis and Kaplan runners is of the order of 0.3 - 0.4 m. Test installations should fulfill the IEC requirements regarding their capacity.

As an example, a view of one of the IMHEF universal test rigs for all types of reaction machines, pumps and turbines is reported in Figure 2. This installation has a 900 kW maximum pumping power, leading to test heads of up to 100 m and a maximum flow rate of 1.4 m^3/s. The dynamometer is limited to a 320 kW maximum generated power at 2 500 rpm.

In general a test procedure consists in measuring

- The overall hydraulic characteristic of the machine and the corresponding efficiency hill chart over a wide range of operating conditions;
- Guaranteed operating point efficiencies and power output;
- Runaway speed;
- Cavitation characteristics;
- Pressure changes at the draft tube inlet, at the spiral case inlet and on the head cover of the machine;
- Flow velocity distribution in various locations.

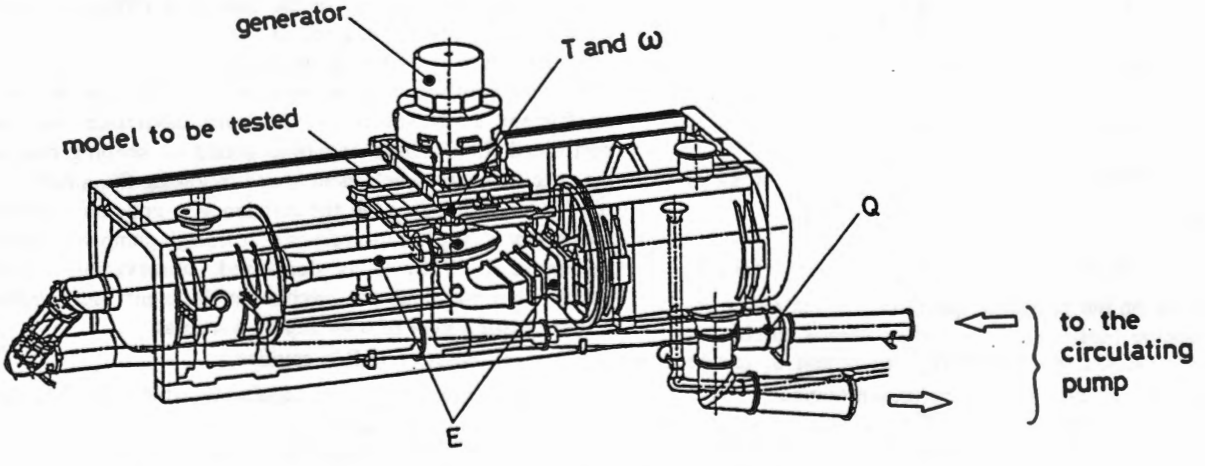

FIG. 2 MODEL OF A FRANCIS TURBINE INSTALLED ON THE IMHEF UNIVERSAL TEST RIG #1.

In addition, mechanical measurements are often carried out, such as torque and bending moment on guide vanes, runner axial thrust etc....

A hill chart corresponding to the model test of a typical Francis hydro-turbine is reported in Figure 3.

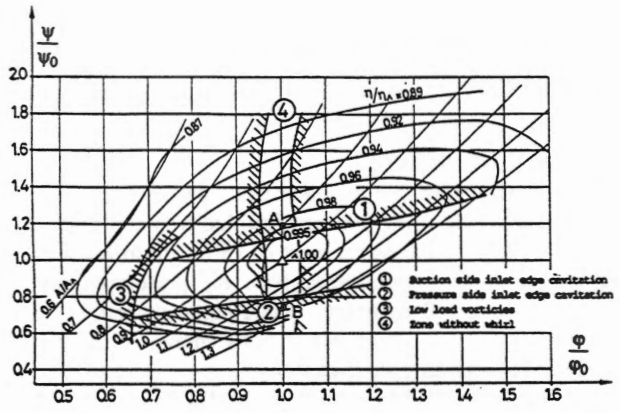

FIG. 3 HILL CHART OF A TYPICAL FRANCIS TURBINE.

Standard cavitation tests

Standard cavitation tests consists in investigating the influence of cavitation development on the hydraulic characteristics of the hydraulic machine and in evaluating the erosion risk. These investigations are very important for the evaluation of the setting level H_s of the machine to the tail-water level Z_a, as shown in Figure 1. Accordingly cavitation tests justify the use of a test rig since the setting level of the machine cannot be varied in the plant. According to the IEC, the Net Positive Suction specific Energy, NPSE, of a hydraulic machine is the difference of the absolute specific energy at Section 2, with the specific energy due to the vapor pressure p_{va}, referred to the reference level Z_r of the machine.

$$NPSE = \left[\frac{p_2}{\rho} + gZ_2 + \frac{C_2^2}{2}\right] - \frac{p_{va}}{\rho} - gZ_r \qquad (Jkg^{-1})$$

Or by introducing the setting level H_s of the machine.

$$H_s = Z_r - Z_a \qquad (m)$$

NPSE can be derived as follows for a turbine,

$$NPSE = \frac{p_a}{\rho} - \frac{p_{va}}{\rho} - gH_s + \frac{C_2^2}{2} \qquad (Jkg^{-1})$$

and for a pump

$$NPSE = \frac{p_a}{\rho} - \frac{p_{va}}{\rho} - gH_s \; . \qquad (Jkg^{-1})$$

Depending on the reference quantities chosen either the Thoma's cavitation coefficient σ, so called Thoma number, or the net positive suction specific energy coefficient ψ_c can be chosen to define a non dimensional cavitation number.

$$\sigma = \frac{NPSE}{E} \; , \psi_c = \frac{2NPSE}{\omega^2 R^2}$$

In both cases, we can observe that these terms are simply related to the setting level H_s which is easily determined. However, the problem arises in estimating the static pressure at the low pressure section c of the runner. The mean specific energy conservation law between these sections leads to the following expression of the absolute pressure p_c,

$$\frac{p_c}{\rho} - \frac{p_{va}}{\rho} = NPSE + g(Z_r - Z_c) - \frac{C_c^2}{2} + \Delta gH_{rc\text{-}2} \qquad (Jkg^{-1})$$

where $\Delta gH_{rc\text{-}2}$ is the mean specific energy losses between the sections c and 2 in the draft tube. According to the flow direction, these losses are positive for a turbine and negative for a pump.

The corresponding dimensionless expression allows to introduce a local cavitation coefficient χ_E related to σ as follows

$$\chi_E = \frac{p_c - p_{va}}{\rho E} = \sigma + \frac{1}{Fr^2}\frac{(Z_r - Z_c)}{D} - \frac{C_c^2}{2E} + \frac{\Delta\psi_{rc\text{-}2}}{\psi}$$

where the Froude number is defined as

$$Fr = \sqrt{\frac{E}{gD}}$$

The necessary condition of cavity onset $p = p_{va}$ in the runner is then expressed by the condition $c_p = -\chi_E$ with the pressure coefficient defined as follows:

$$c_p = \frac{p - p_c}{\rho E}$$

Thus, it is obvious that the static pressure will strongly depend on the operating point of the machine, even though the Thoma number is kept constant. This can be shown by introducing the discharge coefficient φ of the machine. For a turbine we have

$$\chi_E = \sigma + \frac{1}{Fr^2}\frac{(Z_r - Z_c)}{D} - \frac{\varphi^2 + (1 - \frac{\varphi}{\varphi_0})^2}{\psi} + \frac{\Delta\psi_{rc\text{-}2}}{\psi}$$

where φ_0 corresponds to the discharge operation without whirl. For a pump with a pure axial inlet flow, we have in the same way

$$\chi_E = \sigma + \frac{1}{Fr^2}\frac{(Z_r - Z_c)}{D} - \frac{1}{k^2}\frac{\varphi^2}{\psi} + \frac{\Delta\psi_{rc\text{-}2}}{\psi}$$

where k is a pure geometric factor to take into account a given type of reference section. In the case of a reference section taken at the impeller eye, k reduces to unity.

So, in both types of machines the local value of the cavitation coefficient is strongly affected by the discharge coefficient φ. Nevertheless, standard cavitation tests are performed for different operating points by keeping constant the specific energy coefficient ψ and following the influence of the Thoma number σ on the efficiency η and the discharge coefficient φ. Typical η-σ curves of a storage pump are reported in Figure 4. While σ is decreased, observations of the cavitation onset and the cavity development are reported. Characteristic values of σ are reported such as

- σ_i: onset of visible cavities,
- σ_0: lowest value of sigma for which the efficiency remains unchanged,
- σ_1: 1% drop of efficiency.

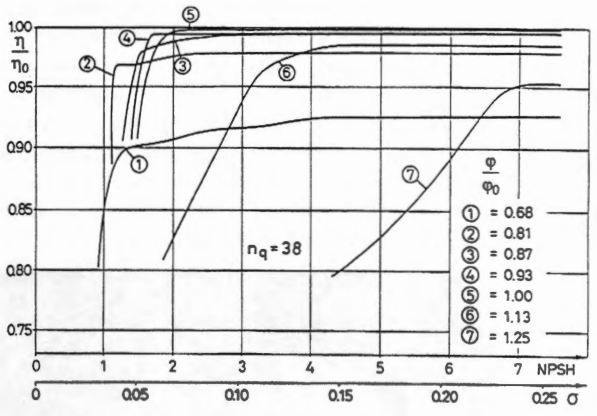

FIG. 4 CAVITATION CURVES OF A STORAGE PUMP.

Froude similitude

Bernoulli's equation written in a steady rotating frame of reference attached to the runner allows us to examine the influence of the Froude number in the case of developed cavitation. Thus for a point of the runner flow passage we have

$$\frac{p}{\rho} + gZ + \frac{W^2}{2} - \frac{U^2}{2} = \frac{p_c}{\rho} + gZ_c + \frac{W_c^2}{2} - \frac{U_c^2}{2} + \Delta gH \ .$$

Or by introducing the pressure coefficient c_p , we obtain the following non dimensional equation

$$c_p = \frac{1}{Fr^2}\frac{(Z_c - Z)}{D} + \frac{1}{\psi}\left[\frac{W_c^2 - W^2}{U_c^2}\right] - \frac{1}{\psi}\left[1 - \frac{U^2}{U_c^2}\right] + \frac{\Delta\psi}{\psi}$$

The cavitation condition $c_p = -\chi_E$ leads to the following relation

$$\frac{1}{Fr^2}\frac{(Z_r - Z)}{D} = -\sigma - \frac{1}{\psi}\left[\frac{W_c^2 - C_c^2 - W^2}{U_c^2}\right] + \frac{1}{\psi}\left[1 - \frac{U^2}{U_c^2}\right] - \frac{\Delta\psi + \Delta\psi_{rc\text{-}2}}{\psi}$$

We can observe that for a given operating point, cavitation tests are in similitude with the prototype flow provided the Thoma numbers and the Froude numbers are the same in both cases, model scale and prototype scale. Owing to the scale length factor between the prototype and the model of large units, it is often impossible to fulfill the Froude similarity requirement. For example, if we consider a runner diameter of 5 m operating at 500 Jkg^{-1} and the runner diameter of the corresponding model being 0.4 m, the Froude similitude leads to a test specific energy of 40 Jkg^{-1} which is too low for testing. Thus, very often the test head is higher than the corresponding Froude head and in turns the cavity vertical extension on the blades is reduced. A way to overcome as much as possible the influence of the Froude number is to choose a reference level of the machine as close as possible to the elevation where cavity development takes place. However, it is strongly recommended to choose the low pressure elevation level gZ_c as reference level since in the case of turbines the drop of efficiency is reached when the cavity development extends up to the runner outlet.

CAVITATION OF HYDRAULIC MACHINES

Influence of the setting level

The objective of cavitation tests being to determine the setting level of the machine in order to overcome any efficiency alteration and to minimize the erosion risk, each type of cavitation is considered with respect to its dependence on the value of the setting level and to the erosion danger.

On the one hand, the onset of a leading edge cavity is more influenced by the blade geometry and the flow incidence angle than the value of σ. This means that increasing to a very high value of σ in order to prevent a leading edge cavity development will cause unacceptable costs. Thus this type of cavity which cannot be avoided for off-design operation has to be considered with respect to the erosion risk. In this case the Thoma number is determined according to an acceptable cavity development.

On the other hand, cavity development corresponding to the design operating point such as bubble cavitation and hub cavity are very sensitive to the Thoma number value. However, for each case of hydraulic machine, different types of cavitation arise depending either on the blade design and the operating point or on the Thoma number value. Thus it is important to examine, for each case of hydraulic machine, the type of cavitation which occurs in the operating range.

Francis turbines

In the case of a Francis turbine and for the design operating range, the type of cavity developing in the runner is closely driven by the specific energy coefficient ψ, the flow coefficient φ influencing only the cavity whirl.

High and low values of ψ correspond to a cavity onset at the leading edge suction side and pressure side of the blades respectively, see Figure 5. This type of cavitation is not very

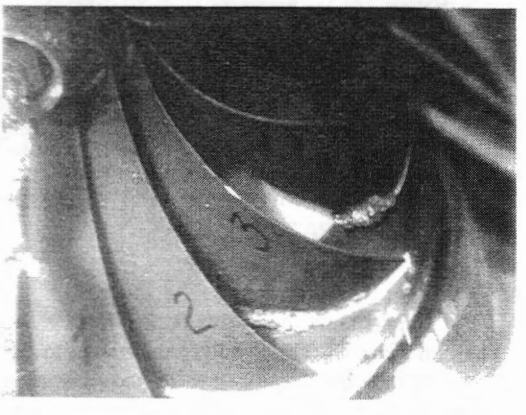

FIG. 5 INLET EDGE CAVITATION, FRANCIS TURBINE.

sensitive to the value of the Thoma number and it can lead to a severe erosion of the blades.

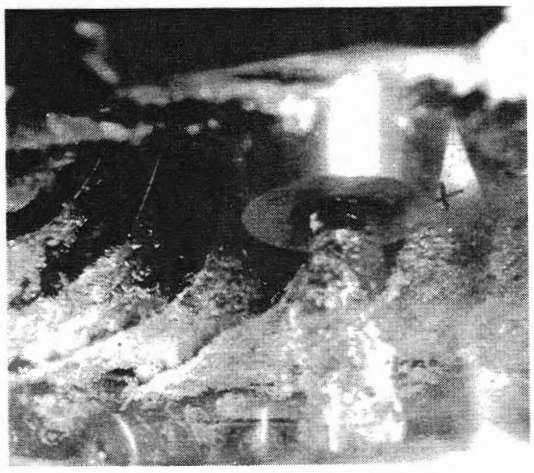

FIG. 6 TRAVELING BUBBLE CAVITATION.

Traveling bubble cavitation takes place for the design value of ψ, at the throat of the runner flow passage, close to the outlet and corresponds to low flow angles of attack. This type of cavitation, illustrated in Figure 6, is very sensitive to the content of cavitation nuclei and to the value of the Thoma number. For this reason the plant NPSE is determined with respect to this type of cavitation. The drop of the η-σ curve is noticed when cavities extend up to the runner outlet in both types of cavitation.

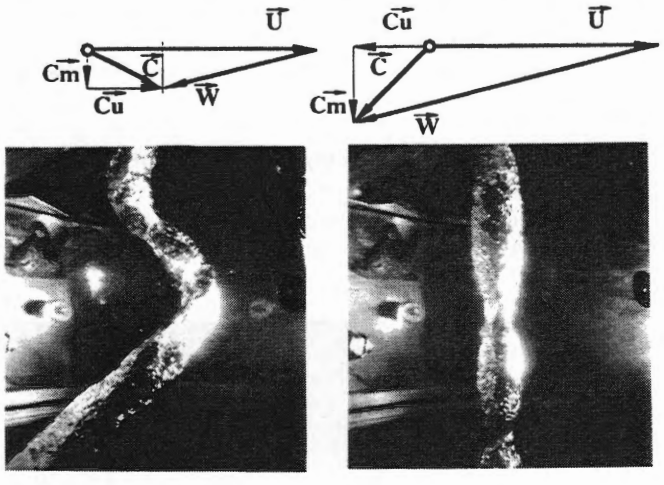

FIG. 7 WHIRL AT LOW AND HIGH DISCHARGE OPERATION.

Depending on the value of the flow coefficient φ, a whirl cavity develops from the hub of the runner to the center axis of the draft tube in the bulk flow, as shown in Figure 7. The size of the cavity is dependent of σ, but the vortex motion depends only on the flow coefficient values. According to the outlet flow velocity triangle of Figure 7, inverse runner rotation of the vortex corresponds to high flow regime and leads to a large axisymmetric fluctuating cavity. In turn, low flow regimes are responsible for a chaotic shape of the whirl, rotating at half the runner rotational speed. The development of such a type of cavity does not cause either erosion or efficiency alteration. The whirl development is mainly concerned with the stability of machine operation, since it is the main source of pressure fluctuations in the hydraulic installation [2].

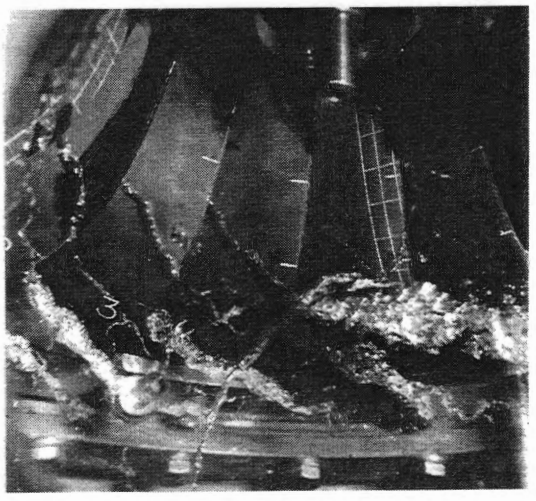

FIG. 8 LOW LOAD CAVITATION VORTICES.

At low load regime, one can observe complex flow recirculation at the inlet of the runner leading to vortex cavitation attached to the hub and extending up to the blade to blade passage, see Figure 8. These low load cavitation vortices can lead to erosion but this type of machine operation is not very frequent since it corresponds to off-design operation.

The different zones in the hill chart corresponding to each type of cavitation onset are reported in Figure 3.

Kaplan and Bulb turbines

Runners of Kaplan and bulb turbines are axial with adjustable blade pitch angle and the control of both the guide vane opening and the blade pitch angle allows optimized operation of the machine, so called "on cam" operation.

For the design operating range a cavity development takes place at the hub of the runner, Figure 9. As this hub cavity reaches the blade trailing edge, we can notice an efficiency drop. This type of cavitation is very sensitive to the Thoma number and determines the plant NPSE of the machine. Any effect of the water cavitation nuclei content is observed for this type of cavitation [3]. However, the air entertainment can have a great influence on the extent of this cavity [4].

Since the blades are adjustable, the runner is not shrouded and then there is a gap between the adjustable blades and the machine casing. As shown in Figure 9, tip clearance cavitation takes place in this gap, leading to an erosion risk

even though the head could be low. This type of cavitation is driven by the flow shear layer in this gap and it is not very dependent of the Thoma number.

FIG. 9 CAVITY DEVELOPMENT IN A KAPLAN RUNNER

Even for the case of on cam operation, leading edge cavities can be observed at the inlet of the runner but could be avoided by improving the shape of the blade leading edge [5]. The different zones in the hill chart corresponding to each type of cavitation onset are reported in Figure 10.

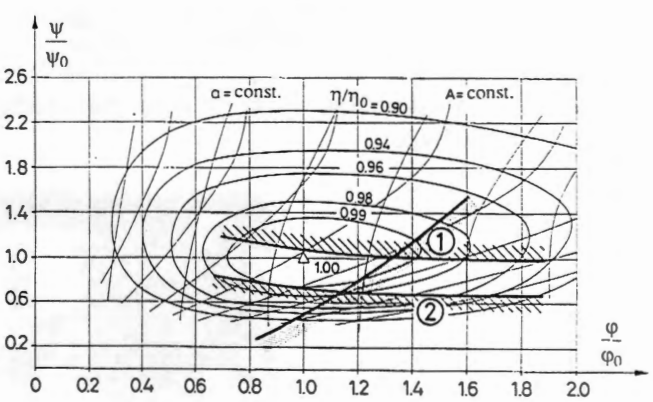

FIG. 10 HILL CHART OF A KAPLAN RUNNER.

Centrifugal pumps

Cavity development in a centrifugal pump is fully controlled by the discharge coefficient. At the rated discharge, bubble cavitation can be observed on the suction side of the blades, see Figure 11. This type of cavity corresponds to a low incidence angle of the flow.

Since the discharge is decreased, the flow incidence is increased and then, a leading edge cavity appears, as shown in Figure 12. Alteration of efficiency is due to the cavity extension up to the throat of the flow passage in the impeller.

But before this efficiency alteration, cavitation erosion can occur at the closure region of the cavity and can be dramatically increased when transient cavities are convected downstream of the impeller throat. For high discharge coefficient value, leading edge cavities are developing at the pressure side of the impeller blades leading to a rapid drop of the efficiency.

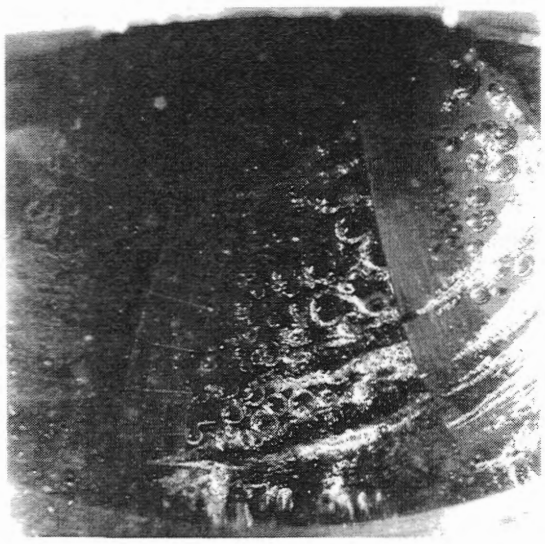

FIG. 11 TRAVELING BUBBLE DEVELOPMENT IN A STORAGE PUMP IMPELLER (DESIGN POINT).

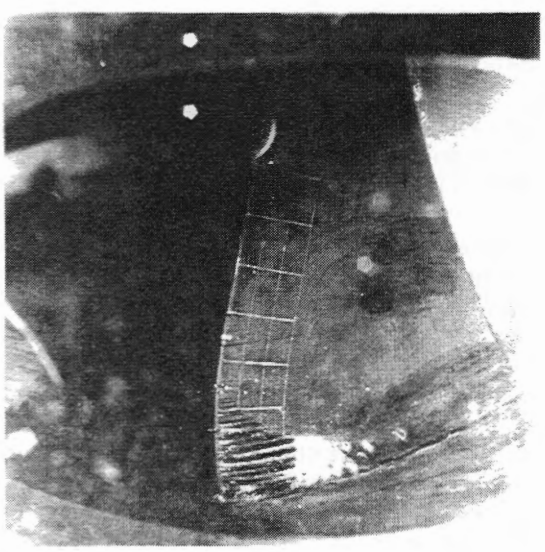

FIG. 12 LEADING EDGE CAVITY IN A STORAGE PUMP IMPELLER.

For low values of σ, cavitation vortices can be observed at the inlet of the runner coming from the leakage flow through the shroud seal. In the case of unshrouded impellers, tip

clearance cavities appear and can erode either the pump casing or the blades themselves.

However, in a centrifugal pump, leading edge cavity is the main type of cavity. Then the setting level of the machine is decided with respect to the erosion risk in the full operating range since for any reasonable value of σ, a leading edge cavity still exists for a sufficiently low value of the discharge coefficient.

FREE STREAM CAVITATION NUCLEI

Free stream cavitation nuclei influence

As it is well known and reported for many years, free gas content is important for the case of traveling bubble cavitation inception. Since 1961, Holl and Wislicenus [6] stated that the volumetric content of critical cavitation nuclei should be λ_L^3 time the content of the field, λ_L being the prototype to model length scale. However, many experiments carried out at IMHEF [7], [8] for different Francis turbines confirm a strong influence of cavitation nuclei content combined with the test head on the efficiency alteration phenomenon by cavitation. Nuclei content does not only influence cavitation inception but also the development of bubble traveling cavities, [9].

Moreover, test head influence is found to be more related to an effect of the active nuclei content than of the Froude effect. According to the Rayleigh Plesset stability analysis the lower radius limit of an active nucleus depends directly on the test head value leading to more or less active nuclei for a given nuclei distribution.

Saturation effect

In Figure 13, taken from [10], cavitation curves correspond to the results of the model of a typical turbine chosen among the wide set of different machines tested at IMHEF. The turbine model is one of the Ataturk turbines [11].

The cavitation curves are obtained according to the usual cavitation tests. In addition, air micro-bubbles are injected in the upstream vessel in order to vary the cavitation nuclei content. It can be observed in Figure 13 that, for a given threshold value of the nuclei content, the efficiency is no longer affected by increasing the nuclei content, the cavitation coefficient being kept constant.

Moreover, the efficiency alteration is strongly related to the cavitation extent on the blade as it is confirmed by flow visualization. Photographs reported in Figure 14, correspond to a test head of 20 m in order to overcome any Froude effect on the cavity extent. Photographs A, B are taken for the same low σ value of 0.052 and correspond to a low nuclei content and to a saturated state, respectively. One can observe that the performance alteration is mainly due to the vaporization of a part of the blade to blade channel region which is under the vapor pressure. Thus, the saturation phenomenon occurs when the active nuclei amount is large enough to occupy all this region.

Similitude of developed traveling bubble cavitation

Evidence of the strong dependency between the volume of vapor and efficiency drop can be found in comparing the photographs B and C, taken for closely the same efficiency drop of 0.2 %. Even though, the sigma value of point C, $\sigma = 0.039$, is rather lower than the σ value of case B, the nuclei content in the case C is small enough to lead to a same volume of vapor and then to the same performance drop.

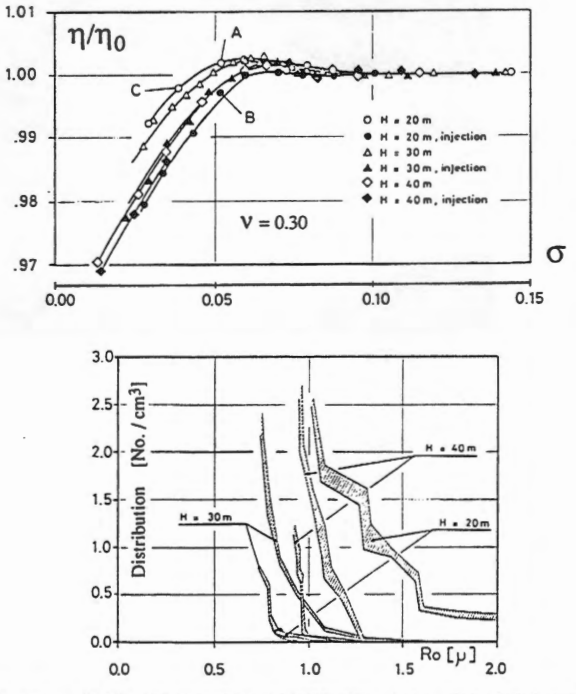

FIG. 13 SATURATION EFFECT ON CAVITATION CURVES.

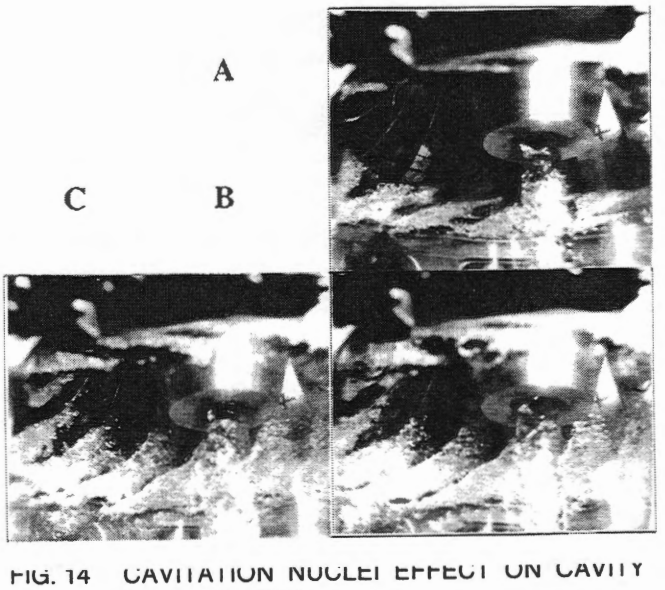

FIG. 14 CAVITATION NUCLEI EFFECT ON CAVITY DEVELOPMENT.

The strong relationship found between cavity extent and efficiency alteration lets us to suggest [12] a modified similitude law for nuclei content based on the total volume occupied by traveling bubble cavitation instead of the number of active nuclei. According to this similitude law, the active nuclei content ratio between the water of the test rig and the water in the prototype turbine should be $\lambda_L^3 \lambda_E^{-3/2}$ if λ_E is the specific energy ratio between the prototype and the model. In addition, the similitude should take into account that the lower radius limit of an active nucleus is scaled by the specific hydraulic energy. Owing to the fact that the saturation state is obtained by injecting cavitation nuclei in the test rig, it is possible to write the necessary condition for saturation in the prototype case. By assuming a n^{th} power law distribution for the radii of the cavitation nuclei, the condition is $1 < \lambda_L^3 \lambda_E^{n-3/2}$ with $10 < \lambda_L < 20$, $1 < \lambda_E < 5$ and $15 < n < 40$.

The consequence is that, if the so called saturation curve is reached on the model for a typical nuclei content of $2\ 10^6$ nuclei/m^3, the corresponding content at the prototype scale has to be of the order of $0.003\ 10^6$ nuclei/m^3. On site measurements [13], confirm that this very low value is always exceeded in the water circulating in the power plant.

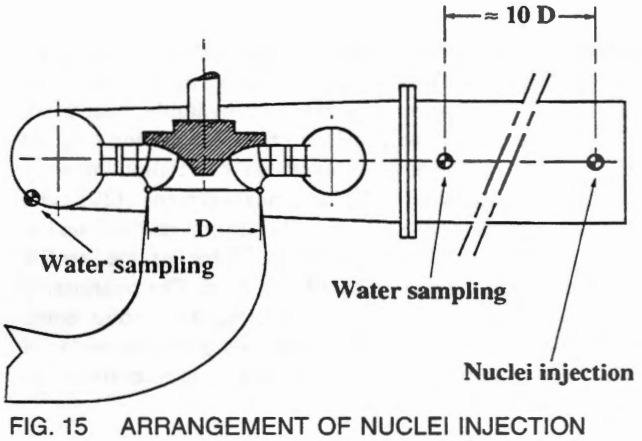

FIG. 15 ARRANGEMENT OF NUCLEI INJECTION AND WATER SAMPLING FOR NUCLEI COUNTING DURING MODEL TESTS.

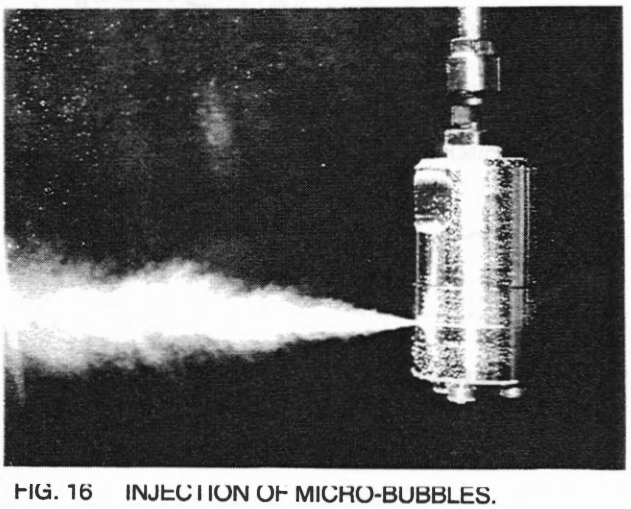

FIG. 16 INJECTION OF MICRO-BUBBLES.

Cavitation test procedure with nuclei injection

Since, for Francis turbines, traveling bubble cavitation at the runner outlet is the type of cavitation used for determining the machine setting level, it is important to have reliable model cavitation tests to predict the full-scale cavitation characteristics. Thus similar cavitation development in the model and the prototype should be obtained. Since the so-called model cavitation saturation characteristic corresponds to the full-scale characteristic, it is, then, necessary to obtain this saturation characteristic during model tests. This can be achieved by increasing the "active" cavitation nuclei, either by increasing the test head, by injecting nuclei into the water, or by using non-degassed water.

Increasing the head to activate more nuclei, can cause unacceptable distortions in the cavitation development if the Froude similitude is not respected, even though a proper reference level of the turbine is chosen. Such a distortion can be observed in Figure 13 by comparing the saturation characteristic for 20 m, 30 m and 40 m test head.

Investigation of a possible way to increase the nuclei content by performing cavitation tests with high dissolved gas content in the water shows that a high gas content does not mean high cavitation nuclei content, and does not lead to the required saturation characteristic, [14]. Moreover, two-phase flow can result from these water conditions, which can affect the stability and the accuracy of the hydraulic parameter measurements.

Thus, it is preferable to seed cavitation nuclei into the test rig at the inlet of the machine according to the arrangement proposed in Figure 15. The system of cavitation nuclei injection developed by IMHEF and systematically used consists in producing micro-bubble by a rapid expansion of air saturated water through very small orifices [15]. The pressure drop into these orifices leads to a cavity development at the outlet and it results in the formation of micro-bubbles, as it can be observed on the photograph of Figure 16. The mean diameter of the generated micro-bubbles depends only on the outlet back pressure which corresponds to the actual test rig pressure. In the pressure range of $0.5\ 10^5$ Pa to $11\ 10^5$ Pa the mean diameter lies between 16 µm and 9 µm, the volumetric nuclei content being as much as $0.5\ 10^{12}$ nuclei/m^3 for an injection flow rate of $21\ 10^{-6}$ m^3/s. Owing to the special mechanical arrangement, up to 16 injectors can be stacked together in order to match the required nuclei content to achieve the saturation state.

However, it is of prime importance to measure the nuclei distribution to check the quality of the test rig, as the active nuclei govern the whole cavitation development process. A special counting technique based on the Venturi nuclei counter, see [12], is now available and well suited for the purpose of hydraulic machine testing. The sampled test water is

accelerated into a Venturi with an adjustable center body, see Figure 17. The acceleration of the flow at the throat leads to an explosive growth of the nuclei which is detected by a piezo electric accelerometer. A pulse counter connected to the accelerometer provides the number per time unit of exploding nuclei. Simultaneous measurements of the upstream pressure and the discharge in the Venturi leads to the computation of the pressure at the throat and thus to the critical pressure of the smallest detected nuclei. The nuclei radius distribution is determined by varying the discharge through the rotational speed of the sampling pump. The center body is adjustable in order to cover a wide range of test heads from 5 m up to 100 m.

Based on all the IMHEF investigations on nuclei content influences on developed cavitation, it appears that the best way to perform cavitation tests is to use a test head as close as possible to the Froude similarity head and to inject nuclei until the cavitation saturation characteristic is reached. However, the test head should be high enough in order to fulfill as much as possible the dynamic homology with the prototype flow. For this reason, the reference level should be taken at the low pressure section c of the runner.

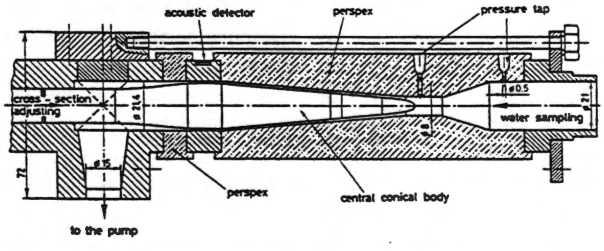

FIG. 17 SKETCH OF THE VENTURI OF THE IMHEF CAVITATION NUCLEI COUNTER.

EROSION RISK

Actual evaluation of cavitation erosion risk

Up to now, erosion risk is subjectively evaluated by considering the cavity development as related to the cavitation type, to the cavity size and to the actual net head of the prototype. Inlet edge cavitation is more erosive than traveling bubbles. Larger cavities lead to more important damage than smaller cavities and, obviously, high head machines are more sensitive to the erosion risk than low head machines, since local velocities are higher. Hydraulic machine manufacturers used to define a "safety" margin as related to the cavitation erosion risk. However, this empirical margin, taken between the σ plant and the σ_0 or σ_1 values determined during the cavitation tests, mixes two completely different physical phenomena, cavitation erosion and efficiency alteration due to the cavity development.

A preferable procedure based on flow visualization is followed by considering the cavity length as a measure of the cavitation "intensity". The erosion risk evaluation is then related to the decision of which cavity extent on the blades is acceptable for a given time operation for the considered operating point and the blade material [16]. This empirical erosion prediction procedure is based on statistical erosion data and takes into account material properties. Cavity length measurements does not require any supplementary instrumentation other than those used for current flow visualization tests i.e. stroboscopic light, camera, windows in the cone and marked blades. Cavity length measurements can be tedious if an image processing software is not used. However flow visualization is the surest way to control the cavitation behavior of the runner and should always be performed.

Paint erosion tests can be used in complement to determine the extent of the eroded area downstream of the leading edge cavity or to examine any possible erosion on the non visible pressure side of the blades. Moreover, this technique allows to determine the blade area to protect with a resistant alloy overlay. Paint erosion tests require that the paint is soft enough to be sensitive to the cavitation attack but resists to the washing of the flow. Repeatability of the tests leads to a rigorous protocol in cleaning the blade surface, in painting, and drying.

Vibratory characteristics of cavitation erosion

Past recent research has shown that a vibratory approach allows to detect cavitation erosion in hydraulic machines, [17], [18]. Extensive studies of the cavitation erosion of a 2D NACA profile [19] show an excellent correlation between direct electrochemical erosion measurement [20] and acceleration levels, above 10 kHz. The erosion rate is found to be proportional to the mean square value of the profile acceleration signal in the 15 to 30 kHz band. The relationship between cavitation erosion and high frequency solid borne noise is also confirmed on both model and prototype scales of turbines. This allows to propose this technique to evaluate the erosion risk.

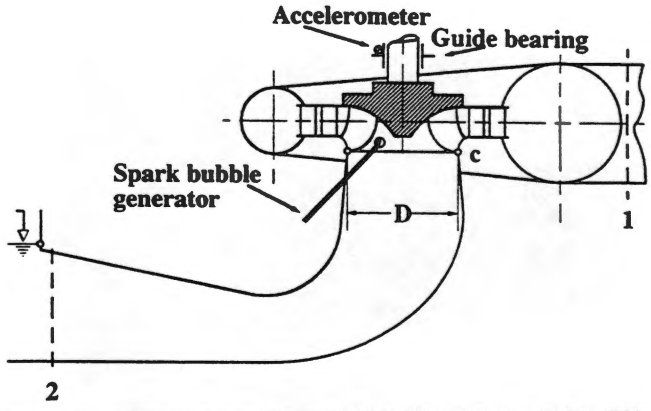

FIG. 18 VIBRATORY DETECTION OF CAVITATION ON THE LOWER GUIDE BEARING.

The procedure consists in installing a high frequency accelerometer as "close" as possible to the runner subjected to cavitation erosion. In this case proximity should be examined in minimizing the pathway of the solid borne noise. Bourdon, [21], shows that measuring acceleration with a sensor placed on the stationary part of the lower guide bearing is equivalent to that placed on the hub of the rotating runner, provided the transmissibility function between the blades and the actual location of the sensor is determined, as it is reported in Figure 18. An impulse force hammer can be used to determine this transmissibility function by hitting successively each blade. Obviously, this is done in air and the water added mass effect on the runner should be taken into account. An instrumented bubble spark generator developed at IMHEF allows to provide short pressure pulses in order to complete the impulse force hammer data. After calibration, it can be used in water to overcome the problem in evaluating the water added mass. Morever, the frequency range of excitation is extended as it is shown by the energy spectrum reported in Figure 19. This spectrum is calculated from the 50 kHz low pass filtered signal of a Bruel and Kjaer hydrophone, type 8103, located at 0.2 m from the spark center. The corresponding photograph of the shock wave taken 5 10^{-6} s after the spark ignition is given in Figure 20.

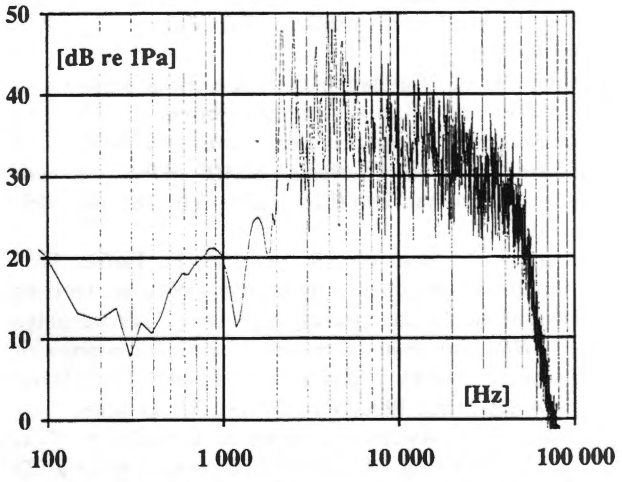

FIG. 19 ENERGY SPECTRUM OF THE SPARK PRESSURE IMPULSE.

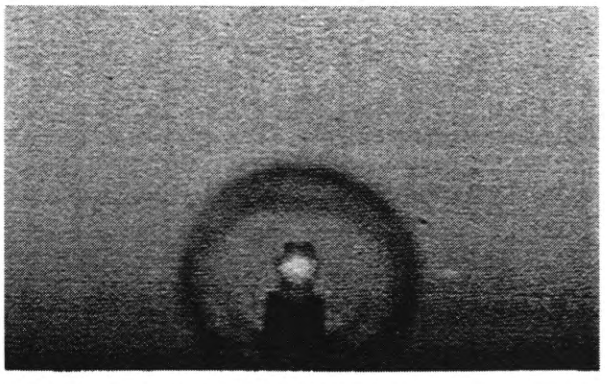

FIG. 19 SPARK IGNITION SHOCK WAVE.

The transmissibility function allows to infer forces or pressure acting on the blades and thus to provide the load induced by cavitation. This load can be then transposed to the prototype scale by using the law derived from the concept of mean erosive power of cavitation [22]. For the two homologous operating points the inferred force would be scaled by the term $\lambda_L^2 \lambda_E^{3/2}$. In the case of the experiment described in [21] , the length scale λ_L between the model and the prototype is 13.2 and the energy scale λ_E is 2.2, leading to a theoretical ratio of 575 for the acting forces on the runner. However the measurements leads to 4N RMS inferred forces on the model and 3 750 N RMS on the prototype which is not so far from the theoretical value of 2 300 N RMS, owing to the fact that the spiral casing of the model was different from the prototype spiral case.

However, the advantage of the vibratory measurement is to define the aggressiveness of a given cavitation development in terms of mechanical engineering units which defines a loading of the materials that metallurgist can include in their own erosion model. Indeed this new procedure has to be validated and refined in different cases, but appears to be very promising.

CONCLUSION

Cavitation tests of hydraulic machines can take benefits from the recent progress made on the studies of the cavitation influence with respect to their hydraulic performance and the erosion risk. The accuracy of the setting level determination of a machine can be improved in a large extent by controlling the cavitation nuclei content of the test water. Procedure and instrumentation already exist to achieve this cavitation nuclei control. Moreover, a relevant indirect method, such as measurement of vibratory levels, can be very useful during the current practice of cavitation tests in order to evaluate the cavitation erosion risk.

ACKNOWLEDGMENT

The author is particularly grateful to the members of the IMHEF Cavitation Research Group, to the technical staff of the IMHEF Test Facility Group and to Prof. P. HENRY. The author wishes also to acknowledge the help of P. BOURDON and R. SIMONEAU of the HYDRO QUEBEC Research Center. This research is financially supported by the Swiss Federal "Commission d' Encouragement à la Recherche Scientifique", the Swiss Energy Producers Association "Nationaler Energie Forschung Fonds", Sulzer Brothers and Hydro Vevey .

REFERENCES

[1] Henry, P., "Hydraulic machine model acceptance tests", *Proceedings of an International Conference on Hydropower Plant*, Water Power '85, Las Vegas, 1985, vol 2, pp. 1258-1267.

[2] Jacob, T., Prenat, J. E.; "Generation of hydro-acoustic disturbances by a Francis turbine model and dynamic behavior analysis", *Proceedings of IAHR 15th Symposium on Modern Technology in Hydraulic Energy Production*, Vol. 2, paper T4, Belgrade, Yugoslavia, 11-14 September 1990.

[3] Gindroz, B., Avellan, F., "Règles de similitude dans les essais de cavitation", *Comptes rendus des XX^{e} Journées de l'Hydraulique de la Société Hydrotechnique de France*, Papier I.18, pp. 1 - 8, Lyon (France), avril 1989.

[4] Strohmer, F., Nichtawitz, A., "Influence of the dissolved air content and head on cavitation test of bulb turbine", *Proceedings of 14th I.A.H.R. Symposium on Hydraulic Machinery: Progress within Large and High Specific Energy*, pp. 779, 786, Trondheim (Norway), June 1988.

[5] Favre, J. N., Avellan, F., Ryhming, I. L., "Cavitation performance improvement by using a 2-D inverse method of hydraulic runner design", *Proceedings of International Conference on Inverse Design Concepts and Optimization in Engineering Sciences-II (ICIDES)*, pp.15-1, 15-15, Pennsylvania State University (USA), October 1987.

[6] Holl, J. W., Wislicenus, G. F.; "Scale effects on cavitation", ASME, Journal of basic Engineering, pp 385-398, 1961.

[7] Henry, P, "Influence of the amount of bubble nuclei on cavitation tests of a Francis turbine", *Proc. of the ASME Symposium, Cavitation and Polyphase Flow Forum*, pp. 23-28, Fort Collins, 12-14 June 1978.

[8] Henry, P., Lecoffre, Y., Larroze, P. Y.; "Effets d'échelle en cavitation", *Proc. of 10th I.A.H.R. Symposium*, pp 103-114, Tokyo, 28 September - 2 October 1980.

[9] Avellan, F., Henry, P.; "Theoretical and experimental study of the inlet and outlet cavitation in a model of a Francis turbine", *Proceedings of 12th I.A.R.H. Symposium on Hydraulic Machinery in the Energy Related Industries*, paper 1-3, pp 38-55, Stirling, August 1984.

[10] Avellan, F., Gindroz, B., Henry, P., Bachmann, P., Vullioud, G., Wegner, M.; "Influence de la chute d'essai et de la nucléation sur les performances en cavitation des modèles de turbines Francis", *Proceedings of 13th I.A.H.R. Symposium on Progress in Technology*, vol. 1, pp 2.1-2.15, Montréal, September 1986.

[11] Henry, P.; *"Turbomachines hydrauliques. Choix illustré de réalisations marquantes"*, Presses polytechniques et universitaires romandes, 412pages, Lausanne, 1992.

[12] Gindroz, B., Avellan, F., Henry, P.; "Similarity rules of cavitation tests: the case of the FRANCIS turbine", *Proceedings of 14th I.A.H.R. Symposium on Hydraulic Machinery: Progress within Large and High Specific Energy*, pp. 755, 766, Trondheim (Norway), June 1988.

[13] Gindroz, B., Henry, P., Avellan, F.; "Francis cavitation tests with nuclei injection", *16th Symposium of the IAHR section on Hydraulic Machinery and Cavitation*, São Paolo (Brazil), 14-18 September 1992.

[14] Gindroz, B., Avellan, F., Henry, P.; "Guide lines for performing cavitation tests", *Proceedings of IAHR 15th Symposium on Modern Technology in Hydraulic Energy Production*, Vol. I, paper H1, 11 pages, Belgrade, Yugoslavia, 11-14 September 1990.

[15] Brand, C., Avellan, F.; "The IMHEF system for cavitation nuclei injection", *16th Symposium of the IAHR section on Hydraulic Machinery and Cavitation*, São Paolo (Brazil), 14-18 September 1992.

[16] Gülich, J. F., "Guidelines for cavitation damage prediction", *Electric Power Research Institute GS-6398 Final Report: Guidelines for Prevention of Cavitation in Centrifugal Feedpumps*, Annex A, November 1989.

[17] Bourdon, P., Simoneau, R., Lavigne, P., "A vibratory approach to the detection of erosive cavitation", *Proc. of International Symposium on Cavitation Noise and Erosion in Fluid Systems, ASME Winter Annual Meeting*, San Francisco (USA), FED: Vol. 88, Dec 1989, pp 95-102.

[18] Abbot, P.A., "Cavitation detection measurements on Francis and Kaplan Hydroturbines", *Proc. of International Symposium on Cavitation Noise and Erosion in Fluid Systems, ASME Winter Annual Meeting*, San Francisco (USA), FED: Vol. 88, Dec 1989, pp 103-109.

[19] Bourdon, P., Simoneau, R., Avellan, F., Farhat, M.;" Vibratory characteristics of erosive cavitation vortices downstream of a fixed leading edge cavity ", *Proceedings of IAHR 15th Symposium on Modern Technology in Hydraulic Energy Production*, Belgrade, Yugoslavia, 11-14 September 1990, Vol. I, paper H3, 12 pages.

[20] Simoneau, R, Avellan, F., Kuhn de Chizelle, Y.; "On Line Measurement Of Cavitation Erosion Rate on a 2D NACA Profile", *Proceedings of 3rd International Symposium on Cavitation Noise and Erosion in Fluid System* of the ASME Winter Annual Meeting, pp. 95-102, San Francisco (USA), December 1989.

[21] Bourdon, P., Simoneau, R., Avellan, F., "Hydraulic turbine cavitation pitting detection by monitoring runner vibration", Final Research Report 307 G 657, submitted to the Canadian Electrical Association, December 1992.

[22] Avellan, F., Dupont, Ph.,Farhat, M.; "Cavitation Erosion Power", *Proceedings of the First ASME-JSDME Fluids Engineering Conference*, FED-Vol. 116, pp. 135-140, Portland, Oregon, USA, 23-27 June 1991.